

# The Relation between Structure and Ferroelectricity in Lead Barium and Barium Strontium Niobates

BY M. H. FRANCOMBE

*Communication from the Staff of the Research Laboratories of The General Electric Company Limited, Wembley, England*

(Received 15 October 1958 and in revised form 9 June 1959)

X-ray crystallographic studies have been made of barium metaniobate,  $\text{BaNb}_2\text{O}_6$ , and of the ferroelectric solid solution series  $(\text{Pb}, \text{Ba})\text{Nb}_2\text{O}_6$  and  $(\text{Ba}, \text{Sr})\text{Nb}_2\text{O}_6$ .  $\text{BaNb}_2\text{O}_6$  possesses two polymorphic structures—a hexagonal form stable within a narrow temperature range below the melting point, 1450 °C., and an orthorhombic form stable at lower temperatures. The single-phase  $(\text{Pb}, \text{Ba})\text{Nb}_2\text{O}_6$  and  $(\text{Ba}, \text{Sr})\text{Nb}_2\text{O}_6$  solid solutions have structures which, like the ferroelectric phase of  $\text{PbNb}_2\text{O}_6$ , are closely related to that of the tetragonal tungsten bronzes, e.g.  $\text{K}_{0.57}\text{WO}_3$ .

In the compounds  $(\text{Pb}_{1-x}\text{Ba}_x)\text{Nb}_2\text{O}_6$  with  $x < 0.4$  the polar axis lies in the direction of one of the  $\langle 110 \rangle$  axes of the related tetragonal structure, and in the ferroelectric phase this produces a slight orthorhombic distortion. High-temperature X-ray studies suggest that as  $x$  exceeds 0.5 the polar axis switches to the unique, short [001] axis of the structure. These ferroelectric strain effects have been attributed to the perovskite-like groups of atoms which form a part of the true repeat unit of the structure. Materials in the range  $0.375 < x < 0.475$  comprise both orthorhombic and tetragonal ferroelectric phases, characterised for each composition by a common Curie point.

The properties of the system  $(\text{Ba}_{1-x}\text{Sr}_x)\text{Nb}_2\text{O}_6$  are broadly similar to those of the  $(\text{Pb}, \text{Ba})\text{Nb}_2\text{O}_6$  series, but, except at the Ba-rich end of the system, i.e.  $x < 0.2$ , the Curie points are generally low, and the ferroelectric strain effects are small.

## 1. Introduction

Lead metaniobate,  $\text{PbNb}_2\text{O}_6$ , was first reported as ferroelectric by Goodman (1953), and is of special interest in high-temperature piezoelectric applications because of its high Curie point, 570 °C. Crystallographic studies by the author (Francombe, 1956) revealed that at room temperature there are two polymorphic forms of  $\text{PbNb}_2\text{O}_6$ , namely, a rhombohedral form, stable at temperatures up to 1200 °C., and the ferroelectric orthorhombic form found in materials rapidly cooled from temperatures in excess of 1250 °C. The rhombohedral polymorph will not be discussed further in this paper. The orthorhombic form is conveniently described as pseudo-tetragonal, and later X-ray work by Roth (1957) has shown that it gives rise to a paraelectric structure above 570 °C. which is fully tetragonal.

Recently the electrical and domain properties of single crystals of  $\text{PbNb}_2\text{O}_6$  have been described by Francombe & Lewis (1958a), and it has been demonstrated (Francombe, 1958) that  $\text{PbNb}_2\text{O}_6$  and compounds of the type  $\text{PbO}_x(\text{Nb}_2\text{O}_5)$ , where  $1 \leq x < 3.0$ , are structurally related to the tetragonal tungsten bronzes  $\text{K}_{0.57}\text{WO}_3$  and  $\text{Na}_{0.23}\text{WO}_3$  described by Magnéni (1949a, b). These studies have shown that  $\text{PbNb}_2\text{O}_6$  undergoes only one electrical or structure transition. Thus, on cooling below the Curie temperature, the unit cell becomes orthorhombic because of a ferroelectric strain along one of the two equivalent axes (at right angles to the original tetrad). The geometry

of this strain makes it convenient to describe the structure using axes of reference (the so-called 'monoclinic' axes) which are not the axes of symmetry, and which give a unit cell whose base is a rhomb.

Goodman (1957) has found that the electrical properties of  $\text{PbNb}_2\text{O}_6$  are considerably enhanced when Pb is partially replaced by Mg, Ca, Sr and Ba. Electrical and crystallographic studies have also been made independently in these laboratories of the systems  $(\text{Pb}, \text{Ba})\text{Nb}_2\text{O}_6$  (Francombe & Lewis, 1958b) and  $(\text{Ba}, \text{Sr})\text{Nb}_2\text{O}_6$ . In the present paper the results of structure investigations on these systems and on  $\text{BaNb}_2\text{O}_6$  are described, and the electrical properties of the solid solutions are interpreted in terms of the grouping of the  $\text{NbO}_6$  octahedra in the tungsten-bronze-type structure. A full account of the methods of preparation and dielectric properties will be given in a separate publication.

## 2. Structure of the pure metaniobates, $\text{PbNb}_2\text{O}_6$ , $\text{BaNb}_2\text{O}_6$ , $\text{SrNb}_2\text{O}_6$

### 2.1. Lead metaniobate, $\text{PbNb}_2\text{O}_6$

To facilitate discussion of the structures formed in the systems  $(\text{Pb}, \text{Ba})\text{Nb}_2\text{O}_6$  and  $(\text{Ba}, \text{Sr})\text{Nb}_2\text{O}_6$  it will be useful to recall briefly the main features of the orthorhombic form of  $\text{PbNb}_2\text{O}_6$ . The lattice dimensions at 20 °C. (Francombe & Lewis, 1958a) are

$$a_0 = 17.65, \quad b_0 = 17.91, \quad c_0 = 7.736 \text{ \AA}.$$

The only reflections appearing in the X-ray powder pattern are those for which  $h+k=2n$ , showing that the cell is face-centred,  $C$ . Thus, the structure may be alternatively described using a primitive (pseudo-tetragonal) cell with  $a_m$  and  $c_m$  axial lengths approximately  $1/2$  times the orthorhombic  $a_0$  or  $b_0$  dimensions. The lattice parameters are then

$$a_m = c_m = 12.573, \quad b_m = 2 \times 3.868 \text{ \AA}, \quad \beta = 90^\circ 56'.$$

This unit cell comprises two bronze-type units of the  $K_{0.57}WO_3$  type, stacked above each other in the  $b_m$ -direction, and contains ten  $PbNb_2O_6$  formula units. The doubling of the  $b_m$  (pseudo-tetragonal  $c$ ) dimension probably arises from puckering of the Nb-O-Nb chains along the short axis of the unit cell. Except for this puckering each bronze-type unit of the  $PbNb_2O_6$  structure is approximately the same as the next, taken in the direction of the short axis. The way in which the  $NbO_6$  octahedra are linked together in the (101) plane of this structure is similar to that in the tetragonal structure I (Table 1), which was depicted in Fig. 2 of the earlier paper by Francombe & Lewis (1958a).

There are three possible types of cation site in the tetragonal-bronze framework (Magnéli, 1949a), described as pentagon, tetragon and triangle sites respectively according to their coordination by  $NbO_6$  octahedra. Thus, the bronze-type sub-unit of the  $PbNb_2O_6$  structure contains four pentagon, two tetragon and four triangle sites, and, of these, five out of the total six pentagon and tetragon sites are occupied by  $Pb^{2+}$  ions. The largest, pentagon, sites could accommodate ions such as  $K^+$ ,  $Pb^{2+}$  or  $Ba^{2+}$ , while the smaller tetragon sites may be filled by  $K^+$ ,  $Na^+$ ,  $Sr^{2+}$ , etc. (by analogy with blue tungsten bronze,  $Na_{0.28}WO_3$ ).

We may regard the bronze-type niobates discussed in this paper as forming a family of structures, which are represented by the potassium tungsten bronze described by Magnéli. There are differences between members of this family, however, as regards both crystal symmetry and electrical properties, and an attempt has been made to distinguish between these structures in Table 1.

## 2.2. Barium metaniobate, $BaNb_2O_6$

Polycrystalline samples of  $BaNb_2O_6$  were prepared by firing the mixed carbonate and oxide in platinum boats at  $1300^\circ C$ . for 1 hour in air. X-ray powder photographs, taken with a 19 cm. Unicam camera using  $Cu K\alpha$  radiation, showed a complex diffraction pattern suggestive of low crystal symmetry.

Small single crystals were next produced by fusing the sintered material in a platinum boat at  $1480^\circ C$ . and air-cooling the charge. Two short columnar fragments, showing sharp (straight) extinction in polarized light, were chosen for single-crystal X-ray studies, and part of the remaining crystal debris was

crushed and examined by the X-ray powder method. The powder photographs showed that a slight simplification of the diffraction pattern had occurred, relative to the original ceramic preparation. Single-crystal rotation photographs, taken with a Unicam 6 cm. camera, showed that the symmetry could now be referred to a hexagonal unit cell with dimensions

$$a_0 = 12.05, \quad c_0 = 3.94 \text{ \AA}, \quad c/a = 0.327.$$

By comparing the X-ray powder patterns for the single-crystal and ceramic materials, it became evident that the complex groups of diffraction-lines observed for the low-temperature (ceramic) structure could be derived by splitting from the diffraction lines of the hexagonal form. A study of these splitting effects enabled the main lines of the powder pattern (for the ceramic form) to be indexed on a new orthorhombic, or (ortho pseudo-) hexagonal, unit cell with the dimensions,

$$a_0 = 12.17, \quad b_0 = 20.5, \quad c_0 = 3.94 \text{ \AA}.*$$

Only those reflections for which  $k=2n$  are observed in the X-ray pattern, and the true cell is therefore smaller than this, with a  $b_0$  dimension of  $10.25 \text{ \AA}$  (see Table 1).

The existence of these two crystal forms of barium metaniobate is apparently open to two interpretations. Thus, either two distinct polymorphic structures of  $BaNb_2O_6$  exist (cf.  $PbNb_2O_6$ ), or alternatively a partial loss of one of the oxide constituents occurs on melting, producing an associated structure change. The first of these explanations was tested by subjecting the single-crystal material to prolonged annealing at a temperature of  $1430^\circ C$ ., just below the melting point, and then slow cooling over a period of  $8\frac{1}{2}$  hours to  $1150^\circ C$ . This resulted in complete reversion from the hexagonal to the orthorhombic form, and therefore confirms that  $BaNb_2O_6$  possesses two polymorphic crystal structures.

Recently, thermal studies of  $BaNb_2O_6$  have been made by Roth (1959) which suggest that no phase transition occurs between  $1200^\circ C$ . and the melting point. It would thus appear that the hexagonal structure is stable over a narrow temperature range close to the melting point, and may be retained only by fairly rapid cooling of the melt.

An interesting feature of  $BaNb_2O_6$  is that in both the polymorphic structures the short  $c_0$  dimension is almost exactly equal to that of the tetragonal-bronze-type  $PbO_x(Nb_2O_5)$  structures, where  $1.5 \leq x < 3.0$ , (Francombe & Lewis, 1958a). Although further crystallographic data for  $BaNb_2O_6$  are not yet available, this indicates that the  $NbO_6$  octahedra are probably linked in linear chains parallel to the  $c$ -axis.

\* Since this paper was submitted unit-cell data obtained with single crystals of orthorhombic  $BaNb_2O_6$  have been published by Coates & Kay (1958). These are in close agreement with the values given here for the powdered material, but show that the true  $c_0$  dimension is doubled (i.e.  $c_0 = 7.87 \text{ \AA}$ ),

### 2.3. Strontium metaniobate, $\text{SrNb}_2\text{O}_6$

As for  $\text{BaNb}_2\text{O}_6$ , this compound was prepared by sintering an equimolar mixture of the carbonate and  $\text{Nb}_2\text{O}_5$  at 1300 °C. in air for 1 hour. The X-ray powder pattern for the product was complex and has not so far been indexed. Attempts to grow single crystals from the melt were unsuccessful, owing to loss of strontium oxide at temperatures above 1400 °C.

### 3. The systems $\text{BaO} \cdot x(\text{Nb}_2\text{O}_5)$ and $\text{SrO} \cdot x(\text{Nb}_2\text{O}_5)$ , where $x > 1$

The fact that tetragonal structures of tungsten-bronze type are developed in the system  $\text{PbO} \cdot x(\text{Nb}_2\text{O}_5)$ , where  $1 \leq x < 3$  (Francombe & Lewis, 1958a), suggested that similar structures might be found in the analogous  $\text{BaO} \cdot x(\text{Nb}_2\text{O}_5)$  and  $\text{SrO} \cdot x(\text{Nb}_2\text{O}_5)$  systems. This idea was accordingly tested by firing mixtures of carbonates and oxides corresponding to nominal  $x$  values of 1.5, 2.0, 2.5 and 3.0 in both systems. As with the pure metaniobates the compounds were sintered in platinum boats in air at 1300 °C., and the products were examined by the X-ray powder method.

Tetragonal-bronze-type structures were formed in

both mixed oxide systems, and may be represented by the approximate nominal compositions  $\text{BaO} \cdot 2(\text{Nb}_2\text{O}_5)$  and  $\text{SrO} \cdot 2.5(\text{Nb}_2\text{O}_5)$  respectively. The unit-cell parameters for these compounds are given in Table 1. Slight relative broadening of  $hk0$  reflections with high indices is detected in the powder pattern of the barium compound, which suggests that the symmetry may be lower than tetragonal.

With nominal compositions containing more Ba or Sr the products were two-phase, comprising in each case the metaniobate (i.e.  $\text{BaNb}_2\text{O}_6$  or  $\text{SrNb}_2\text{O}_6$ ) and the bronze-type phase. When the values of  $x$  exceeded those given above uncombined  $\text{Nb}_2\text{O}_5$  appeared in addition to the bronze-type phase.

The formulae of these bronze-type phases may also be written as  $\text{Ba}_{0.25}\text{NbO}_{2.75}$  and  $\text{Sr}_{0.2}\text{NbO}_{2.7}$ , and it would appear that, referred to the ideal  $A_x\text{BO}_3$  bronze formula, the niobate structures must be oxygen-deficient. In Table 1 these phases are therefore described as type III to distinguish them from other tetragonal structures such as types I and IV where the formula indicates a full complement of oxygen ions. No single-crystal data have yet been obtained which would show whether such oxygen defects are ordered in the crystal structure.

Table 1. Phases discussed in present paper (all existent at room temperature except where otherwise stated)

Formula	Symmetry	Cell dimensions (Å)	Electrical state	Symbol for phase
1. $\text{PbNb}_2\text{O}_6$ above 570 °C.	Tetragonal	$a_0 = 12.46, c_0 = 3.907$	Paraelectric	I
2. $\text{PbNb}_2\text{O}_6$ at 20 °C.	Orthorhombic (pseudo-tetragonal)	$a_m = c_m = 12.573, b_m = 2 \times 3.868$ $\beta = 90^\circ 56'$	Ferroelectric, polar axis [101]	II
3. $\text{SrNb}_2\text{O}_6$	?	Not determined	—	$\text{SrNb}_2\text{O}_6$
4. $\text{BaNb}_2\text{O}_6$ quenched	Hexagonal	$a_0 = 12.05, c_0 = 3.94$ $c/a = 0.327$	—	H <sub>1</sub>
5. $\text{BaNb}_2\text{O}_6$ annealed	Orthorhombic	$a_0 = 12.17, b_0 = 10.25,$ $c_0 = 3.94$	—	H <sub>2</sub>
6. $\text{BaO} \cdot 2(\text{Nb}_2\text{O}_5)$	Tetragonal ?	$a_0 = 12.46, c_0 = 3.97$ $c/a = 0.319$	—	III
7. $\text{SrO} \cdot 2.5(\text{Nb}_2\text{O}_5)$	Tetragonal	$a_0 = 12.34, c_0 = 3.94$ $c/a = 0.319$	—	III
8. $\text{Pb}_{1-x}\text{Ba}_x\text{Nb}_2\text{O}_6$ $x = 0$ to 0.45	Orthorhombic (pseudo-tetragonal)	$\left. \begin{array}{l} \text{As } 2. \\ a_m = c_m = 12.53, b_m = 3.925 \\ \beta = 90^\circ 27' \end{array} \right\}$	As 2.	II
9. $\text{Pb}_{1-x}\text{Ba}_x\text{Nb}_2\text{O}_6$ $x = 0.4$ to 0.8	Tetragonal	$\left. \begin{array}{l} a_0 = 12.475, c_0 = 3.95 \\ a_0 = 12.48, c_0 = 3.98 \end{array} \right\}$	Ferroelectric, polar axis probably [001]	IV
10. $\text{Pb}_{1-x}\text{Ba}_x\text{Nb}_2\text{O}_6$ $x = 0.8$ to 1.0	Orthorhombic	As 5.	—	H <sub>2</sub>
11. $\text{Ba}_{1-x}\text{Sr}_x\text{Nb}_2\text{O}_6$ $x \approx 0.15$	Tetragonal	$a_0 = 12.46, c_0 = 3.98$	As 9.	IV
12. $\text{Ba}_{1-x}\text{Sr}_x\text{Nb}_2\text{O}_6$ $x = 0.2$ to 0.45	Tetragonal	$a_0 = 12.45, c_0 = 3.94$	As 9.	IV
13. $\text{Ba}_{1-x}\text{Sr}_x\text{Nb}_2\text{O}_6$ $x = 0.6$ to 0.8	Orthorhombic pseudo-tetragonal ?	$a_0 = 12.41, c_0 = 3.92$	As 2. (?)	II (?)

#### 4. The system $(\text{Pb},\text{Ba})\text{Nb}_2\text{O}_6$

X-ray powder studies were made of ceramic specimens with nominal compositions  $\text{Pb}_{1-x}\text{Ba}_x\text{Nb}_2\text{O}_6$ , where  $0 < x \leq 0.9$ .

For small replacements of Pb (i.e. up to  $x=0.01$ ) no change was detected in the  $\text{PbNb}_2\text{O}_6$  (type II) structure, but the ceramic discs often contained pink crystalline inclusions which were identified as the rhombohedral polymorph of  $\text{PbNb}_2\text{O}_6$ . With  $x \geq 0.05$ , homogeneous type II phases were obtained showing a progressive decrease in the distortion as  $x$  is increased. The effect is depicted graphically in Fig. 1, where the parameters of the primitive bronze-type unit cell are plotted against composition. This shows that as Ba replaces Pb the interaxial angle  $\beta$  falls in value, while the  $a_m$  and  $b_m$  dimensions respectively decrease and increase.

At the composition  $x=0.4$  a second phase appears, closely related to the main phase, but differing from it in possessing a  $\beta$  angle of  $90^\circ$  and slightly different unit-cell dimensions (see Fig. 1). The concentration of this new tetragonal phase increases rapidly from about 15% of the whole for  $x=0.4$ , to 50% for  $x=0.425$  and 95% for  $x=0.475$ . The range over which the orthorhombic and tetragonal phases co-exist appears to extend from about  $x=0.375$  to 0.475.

In the composition range  $0.5 \leq x \leq 0.8$  the tetragonal phase is formed as a solid solution phase; its  $a_T$  lattice parameter shows little or no variation with composition, but the  $c_T$  parameter (equivalent to  $b_m$  for the orthorhombic phase) undergoes a gradual increase. With  $x$  values higher than 0.8 a second phase, orthorhombic  $\text{BaNb}_2\text{O}_6$ , is present, the lattice parameters of the tetragonal phase showing no further change.

To explain the lattice parameter changes shown in Fig. 1 it is necessary to consider three main factors, (a) the influence of replacement of Pb by Ba on the type and magnitude of the crystal distortion, (b) the effect of ionic size difference between  $\text{Pb}^{2+}$  and  $\text{Ba}^{2+}$  ( $r=1.32$  and  $1.43$  Å respectively), and (c) the difference in the type of bonding preferred by Pb and Ba atoms in the bronze-type structure. We shall not attempt a discussion of the first of these factors at this stage, since this forms the subject of a more detailed treatment in Section 8 below. It is possible, however, to interpret the main features of the parameter curves in Fig. 1 by considering factors (b) and (c) in relation to the cation sites available in the tungsten-bronze-type  $\text{PbNb}_2\text{O}_6$  structure.

In  $\text{PbNb}_2\text{O}_6$  it is probable that the marked contraction of the  $b_m$  dimension is produced by strong covalent bonding of Pb in the tetragon sites, of the type found in  $\text{PbO}$ , as suggested by Francombe & Lewis (1958a). The contraction of the structure, and associated puckering of the Nb-O-Nb chains extending along the  $b_m$ -axis, is limited by the fact that the larger pentagon sites are filled with  $\text{Pb}^{2+}$  ions

( $r=1.32$  Å), and can proceed only to the point where the pentagon oxygen rings are close-packed above and below the Pb atoms.

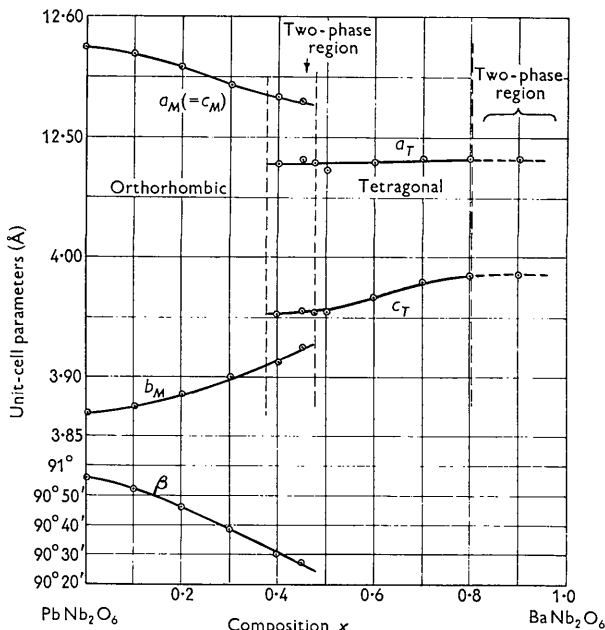


Fig. 1. Variation of lattice parameters with composition for system  $(\text{Pb}_{1-x}\text{Ba}_x)\text{Nb}_2\text{O}_6$ .

If now the  $\text{Pb}^{2+}$  ions in these large sites are replaced by larger  $\text{Ba}^{2+}$  ions the structure is gradually expanded in the  $b_m$ -direction, against the forces exerted by the covalent Pb-O bonds. That there is a strong preference for  $\text{Pb}^{2+}$  ions to remain in tetragon sites is demonstrated by the fact that the limit of replacement of Pb is reached (in this series) at a composition which would allow all four pentagon sites in the bronze-type unit cell to be filled with  $\text{Ba}^{2+}$  ions, the one filled tetragon site still being occupied by Pb (i.e.  $x=0.8$ ). This interpretation is also consistent with the view that the high lattice strain of  $\text{PbNb}_2\text{O}_6$  originates chiefly in the type of bonding preferred by Pb atoms.

#### 5. High-temperature X-ray study

In an effort to understand the effects of temperature on the tetragonal solid solutions of type IV, a high-temperature X-ray powder study was made of the compound  $\text{Pb}_{0.4}\text{Ba}_{0.6}\text{Nb}_2\text{O}_6$ . The results are shown in Fig. 2 (expressed in a form convenient for later discussion). It was found that, although the structure is tetragonal both below and above the Curie point (290 °C.), a discontinuous change in the  $c/a$  axial ratio occurs on passing through the transition temperature. In the powder pattern the 620 and 002 reflections are clearly resolved at temperatures below  $T_c$  (with  $d_{(002)} > d_{(620)}$ ), but are observed to overlap exactly in all photographs taken at temperatures higher than  $T_c$ .

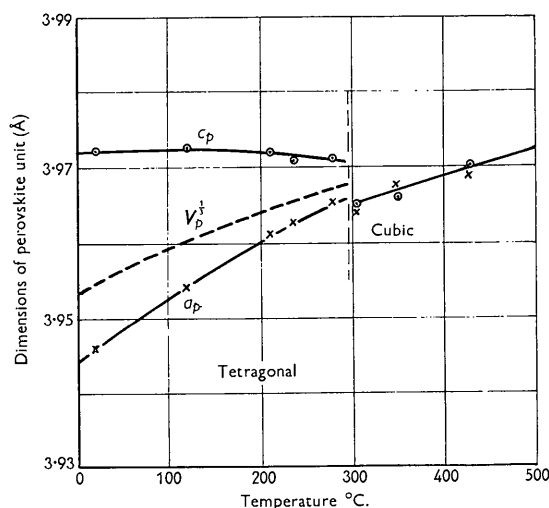


Fig. 2. Variation of dimensions of perovskite sub-unit with temperature in  $\text{Pb}_{0.4}\text{Ba}_{0.6}\text{Nb}_2\text{O}_6$ .

○○○○ Experimental observations of  $d_{(002)} \times 2$ .  
× × × Experimental observations of  $d_{(620)} \times 2$ .

This means that  $c_0$  is greater than  $a_0/\sqrt{10}$  for the ferroelectric phase, and becomes equal to  $a_0/\sqrt{10}$  above the Curie point. Discussion of this will be given in Section 8.

## 6. The system $(\text{Ba}, \text{Sr})\text{Nb}_2\text{O}_6$

Although neither  $\text{BaNb}_2\text{O}_6$  nor  $\text{SrNb}_2\text{O}_6$  possesses a tetragonal-bronze-type structure, it has been established (Section 3) that the compounds  $\text{BaO} \cdot 2(\text{Nb}_2\text{O}_5)$  and  $\text{SrO} \cdot 2.5(\text{Nb}_2\text{O}_5)$  do crystallize in this form. Also the hypothesis advanced in Section 4, that in the  $(\text{Pb}, \text{Ba})\text{Nb}_2\text{O}_6$  solid solution series bronze-type structures are produced in which all or most of the large pentagon cation sites are filled with Ba, suggested that these investigations might profitably be extended to other barium-rich systems such as  $(\text{Ba}, \text{Sr})\text{Nb}_2\text{O}_6$ . Crystallographic and dielectric studies have now been made of the series  $(\text{Ba}_{1-x}\text{Sr}_x)\text{Nb}_2\text{O}_6$ , which show that over a wide composition range a single-phase solid solution of tungsten-bronze-type is formed exhibiting weak ferroelectricity.

The X-ray powder data are shown in Fig. 3. At most compositions, the photographs show evidence of a single tetragonal phase only. There appears to be no appreciable solid solution of  $\text{SrNb}_2\text{O}_6$  in the  $\text{BaNb}_2\text{O}_6$  structure, since even for  $x$  as low as 0.05 the tetragonal phase appears. Above  $x=0.7$ , the  $\text{SrNb}_2\text{O}_6$  phase occurs as well. The cell dimensions of the tetragonal phase do not, however, change uniformly with composition; there are regions near  $x=0.15$  and  $x=0.55$  where rapid variations occur. Whether these represent discontinuities and the entry of new phases, not very different from each other, cannot be decided on this evidence. A reasonable explanation can, however, be given as follows.

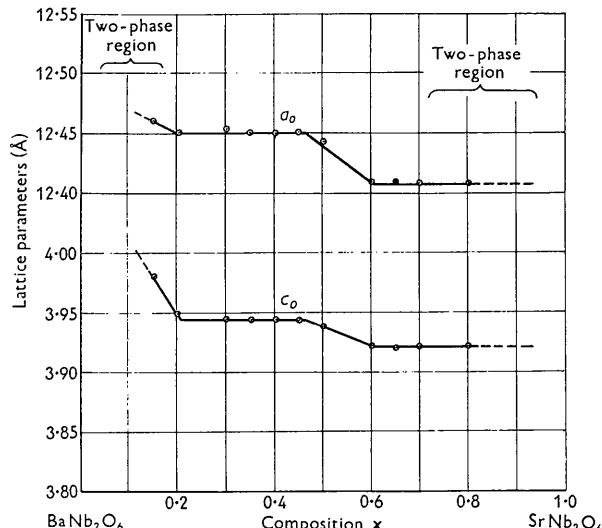


Fig. 3. Variation of lattice parameters with composition for system  $(\text{Ba}_{1-x}\text{Sr}_x)\text{Nb}_2\text{O}_6$ .

The composition  $\text{Ba}_{0.9}\text{Sr}_{0.1}\text{Nb}_2\text{O}_6$  probably corresponds to a cation arrangement where all the pentagon sites are filled with Ba, with equal numbers of  $\text{Ba}^{2+}$  and  $\text{Sr}^{2+}$  ions in the tetragon sites. The marked drop as  $x$  increases to 0.2 is consistent with the replacement of large  $\text{Ba}^{2+}$  ions ( $r=1.43$  Å) by smaller  $\text{Sr}^{2+}$  ions ( $r=1.27$  Å) in tetragon sites. Up to  $x=0.45$  there are probably sufficient  $\text{Ba}^{2+}$  ions close-packed in the large pentagon sites to maintain an almost constant unit-cell volume, and the chains of  $\text{NbO}_6$  octahedra are unpuckered, as suggested by the  $c_0$  dimension of 3.94 Å (Francombe & Lewis, 1957). The change from  $x=0.45$  to 0.6, now corresponding to the appearance of approximately equal numbers of  $\text{Ba}^{2+}$  and  $\text{Sr}^{2+}$  ions in pentagon sites, with  $\text{Sr}^{2+}$  ions in tetragon sites, results in a partial collapse of the structure cell due to the higher concentration of smaller  $\text{Sr}^{2+}$  ions.

The reduction of the  $c_0$  spacing at  $x \approx 0.6$  is presumably associated with puckering of the  $\text{Nb}-\text{O}-\text{Nb}$  chains relative to the  $c$ -axis. For  $x > 0.7$  a further phase of  $\text{SrNb}_2\text{O}_6$ -type appears, and this suggests that the structure with the contracted unit cell ( $c_0=3.92$  Å) probably has only a limited range of composition, extending between  $x=0.6$  and 0.7. For compositions containing more Sr than  $x=0.7$  the  $\text{SrNb}_2\text{O}_6$ -type structure is relatively more stable.

## 7. Electrical properties

Ceramic specimens of the lead-barium and barium-strontium niobates were tested for ferroelectricity by a modified form of the method of Sawyer-Towers, the existence of a hysteresis loop being accepted as a criterion, and the height of the loop giving an estimate of the magnitude of the effect. These dielectric studies will be fully described in a further paper. We shall,

however, summarize briefly what is known about the variation of electrical properties with composition in the two series, before proceeding to discuss in Section 8 the relation between ferroelectricity and crystal structure.

Materials in the system  $Pb_{1-x}Ba_xNb_2O_6$  with  $0 < x \leq 0.45$  are strongly ferroelectric (Franccombe & Lewis, 1958*b*), and are characterized by high values of peak permittivity, electromechanical coupling coefficient and  $Q$ . Curie temperatures, determined from permittivity-temperature plots, fall with increase in Ba content, as shown in Fig. 6, reaching a minimum at about  $x=0.5$ , and then rise again as  $x$  increases to 0.8. An optimum combination of ferroelectric properties appears to be attained at or near the composition  $x=0.4$ ; beyond this point the ferroelectric behaviour progressively deteriorates as the Ba-rich end of the system is approached.

Ferroelectricity in the system  $Ba_{1-x}Sr_xNb_2O_6$  is appreciably weaker than in the system  $Pb_{1-x}Ba_xNb_2O_6$ , and except at the Ba-rich end of the former the Curie points are much lower (Fig. 8). We may divide the phase diagram into three parts in the following way. Thus, at the  $BaNb_2O_6$  side of the diagram there is a limited range of composition near  $x=0.2$  for which Curie points are high, but ferroelectric properties are very weak. Materials between  $x=0.3$  and 0.5 show lower Curie points ( $T_c \approx 100$  °C.) but stronger ferroelectricity than materials with low values of  $x$ . Finally, materials from  $x=0.55$  to  $x=0.7$  have very low Curie points (between about 50 and 80 °C.), but show appreciably improved ferroelectric properties and higher peak permittivities than materials with  $x < 0.5$ .

## 8. Interpretation of ferroelectric strain effects

We now wish to find the connection between the electrical effects and the geometrical strain of the unit cell on cooling below the Curie point. The same type of strain that was found in  $PbNb_2O_6$  (Franccombe & Lewis, 1958*a*) now is found also in Pb-rich compositions of the system  $Pb_{1-x}Ba_xNb_2O_6$ , but the distortion is reduced in magnitude as the value of  $x$  increases. In the lead-barium niobates with  $0.5 \leq x \leq 0.8$ , and also in the barium-strontium niobates, there is no geometrical strain which can be obviously interpreted as the ferroelectric strain. These structures are tetragonal, and it appears impossible for a transformation to occur to any crystal system of higher symmetry on passing through the Curie point. There is, however, the possibility of increased symmetry either by a change of crystal class within the tetragonal system, or by the adoption of a smaller unit cell, both changes which might be difficult to detect in powder photographs. The evidence recorded in Section 5 about the ferroelectric-paraelectric transition of  $Pb_{0.4}Ba_{0.6}Nb_2O_6$  provides a useful starting point, and can be interpreted in the following way.

From the geometry of the tetragonal bronze-type

structure with its regular grouping of  $NbO_6$  octahedra into 3-, 4- and 5-membered rings, it can readily be shown that the distance  $a_0/\sqrt{10}$  is equivalent to the corner-to-corner diameter of an octahedron, or to the shortest Nb-Nb separation, in the (001) plane. Thus, above the Curie temperature the Nb-Nb spacing along the  $c$ -axis (in other words  $c_0$ ) becomes equal to that in the (001) plane.

This equivalence of Nb-Nb distances does not imply that all the octahedra become regular in shape, since this is prohibited by the geometry of their grouping. It does suggest, however, that those atom groups containing the so-called tetragon sites of the lattice are tetragonal in the ferroelectric phase and become cubic above the Curie point. These groups are arranged in the unit cell as shown in Fig. 4, and com-

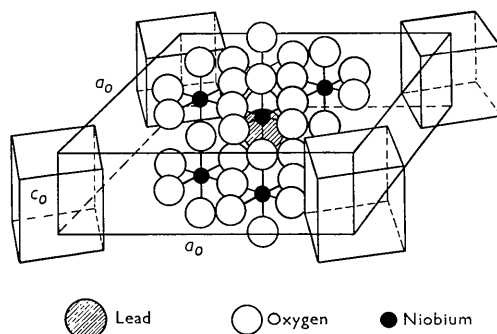


Fig. 4. View of the paraelectric  $PbNb_2O_6$  structure cell showing perovskite-type sub-units.

prise residual fractions of a perovskite structure, but are linked together in a more complex way than in perovskite. We may represent the edge lengths of each such perovskite sub-unit as  $a_p$  in the (001) plane and  $c_p$  in the [001] direction. In terms of the spacings of specific lattice planes they are expressed as follows

$$a_p = a_0/\sqrt{10} = 2d_{(620)}, \\ c_p = c_0 = 2d_{(002)}.$$

As shown in Fig. 2, the removal of the tetragonal distortion at  $T_c$  is achieved through an abrupt relative contraction of the  $c_p$  dimension, and is associated with a slight reduction in the volume of the sub-unit. Thus, although the direction of spontaneous polarization has not been determined by electrical measurements on single crystals, the nature of the structure change strongly suggests that the  $c$ -axis of the structure is the ferroelectric polar axis.

If it is now assumed that the ferroelectric properties of these structures originate in the perovskite-type sub-units, the observed strain effects for the  $(Pb, Ba)Nb_2O_6$  and  $(Ba, Sr)Nb_2O_6$  niobates can be explained in terms of the pseudo-symmetry of these units. Using the lattice parameter data given in Fig. 1 for the lead-barium compounds with orthorhombic structures, it may be shown that  $c_p/a_p$  as defined

above is less than unity. Also, each perovskite unit probably undergoes a shear indicated by the appearance of a strain directed along its face diagonal, as shown in Fig. 5(a). The observed overall strain may then be regarded as originating in the appearance of expansion along  $[110]_p$  (referred to the perovskite axes). The deformation of each unit is thus directly comparable with that produced for example in the orthorhombic phase of  $\text{BaTiO}_3$ .

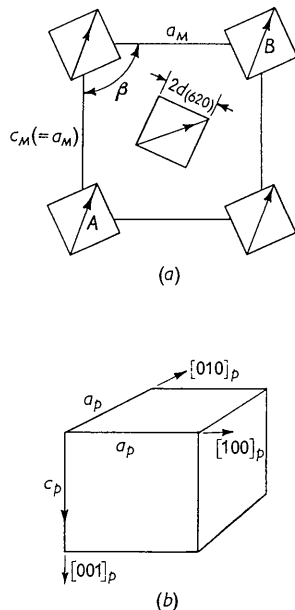


Fig. 5. Directions of ferroelectric strain in perovskite-type sub-units of  $(\text{Pb}_{1-x}\text{Ba}_x)\text{Nb}_2\text{O}_6$  structures.

- (a) Compositions with  $0 \leq x < 0.4$ .
- (b) Compositions with  $0.5 \leq x \leq 0.8$ .

The monoclinic angle  $\beta$  for each composition is less for the perovskite sub-units than for the structure cell containing them. Thus, if the ferroelectric strain of the true unit cell is expressed in terms of the ratio of the orthorhombic parameters  $b_0/a_0$  (i.e.  $2 \tan \beta/2$ ), then the corresponding ratio for the enclosed perovskite sub-units is

$$[a_0 + (b_0 - a_0) \cos \alpha]/a_0,$$

where  $\alpha$  is approximately  $36\frac{1}{2}^\circ$ , and is the angle between the face diagonal of a sub-unit and that of the main bronze-type unit cell (Fig. 5(a)). Similarly, the strain for the tetragonal structures would be proportional to the axial ratio  $c_p/a_p$ , in the same way as for the tetragonal perovskite-type ferroelectrics such as  $\text{BaTiO}_3$  and  $\text{KNbO}_3$ . If both orthorhombic and tetragonal strains are ferroelectric in origin, they should show the same type of variation with composition as the Curie temperature in each solid-solution series. That this condition is fulfilled satisfactorily in the  $(\text{Pb}, \text{Ba})\text{Nb}_2\text{O}_6$  series may be seen by comparing the plot of axial ratios in Fig. 7 with the trend shown by

$T_c$  in the phase diagram, Fig. 6. In Fig. 7 the values of  $b_0/a_0$  for the main orthorhombic cell, and also the smaller ratios for the perovskite sub-units, are shown.

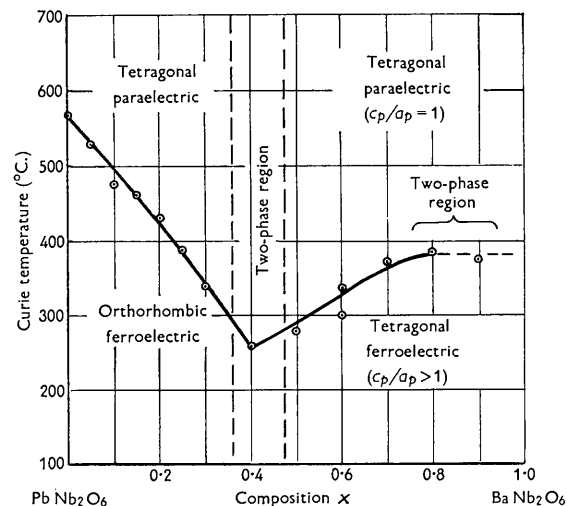


Fig. 6. Phase diagram for ferroelectric solid-solution system  $(\text{Pb}_{1-x}\text{Ba}_x)\text{Nb}_2\text{O}_6$  (compiled from electrical and structural data).

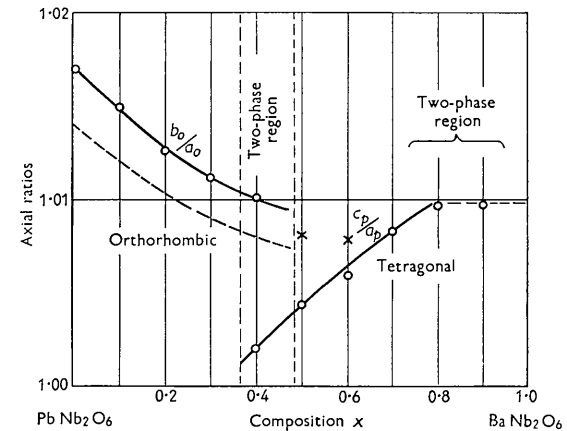


Fig. 7. Axial ratios of  $(\text{Pb}_{1-x}\text{Ba}_x)\text{Nb}_2\text{O}_6$  structures.

- ○ ○ Ceramic samples.
- × × × Single-crystal preparations.
- - - Reduced orthorhombic axial ratios for perovskite sub-units.

Throughout this discussion it has been assumed that the distortions are homogeneous, so that the shape of the sub-units may be deduced from the shape of the cell without detailed information about atomic positions. In the orthorhombic structures, where packing effects and associated puckering of the Nb atoms play a significant role, this assumption might not be justified. For the tetragonal structures, however, where puckering is slight or non-existent, the approach used above probably gives a good approximation.

In the barium-strontium niobates the Curie temper-

atures are low, and the associated crystal strain effects are small. For the composition range  $0.15 \leq x \leq 0.5$  it is possible to correlate the ferroelectric behaviour with a definite tetragonal strain ( $c_p/a_p > 1$ ) within the perovskite units. This is illustrated by comparing the plots of  $T_c$  and  $c_p/a_p$  with composition, shown respectively in Figs. 8 and 9. Thus, for  $x < 0.2$  both the Curie temperature and the tetragonal strain are high, and they show the same sequence of changes with composition as  $x$  increases to 0.7.

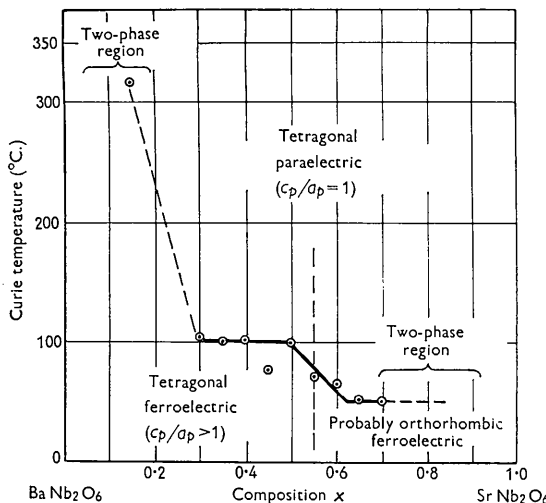


Fig. 8. Phase diagram for ferroelectric solid-solution system  $(\text{Ba}_{1-x}\text{Sr}_x)\text{Nb}_2\text{O}_6$  (compiled from electrical and structural data).

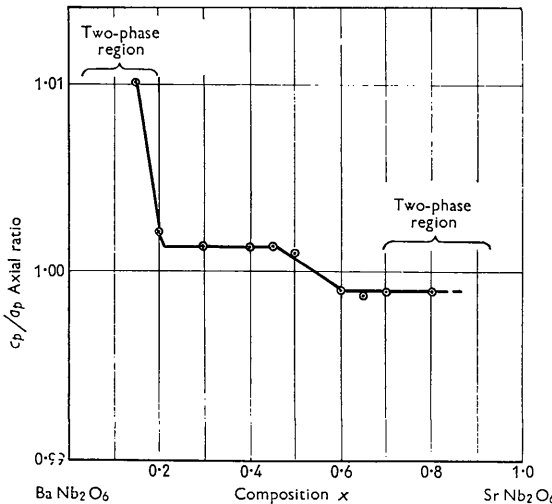


Fig. 9. Variation of  $c_p/a_p$  axial ratio for perovskite sub-units in system  $(\text{Ba}_{1-x}\text{Sr}_x)\text{Nb}_2\text{O}_6$ .

With  $0.5 < x \leq 0.7$  the  $c_p/a_p$  ratio is slightly less than unity, and therefore the tetragonal distortion cannot be directly attributed to ferroelectric strain. By analogy with the Pb-rich compositions in the lead-barium series, this reduction of the  $c_p/a_p$  ratio below

unity may be associated with the appearance of a very small strain reducing the symmetry to orthorhombic. Such a strain has not been observed, but it might be difficult to detect in the X-ray powder photographs because of the low symmetry of the crystal structure. It would be consistent with the very low Curie temperatures in this region, and would also explain why the peak permittivities are uniformly higher at the Sr-rich end of the series. In the orthorhombic structures the resultant polar moment can be directed along either of two directions which, in the related tetragonal structure, are equivalent  $\langle 110 \rangle$  axes, in contrast to the single unique  $[001]$  axis for the tetragonal structures with  $c_p/a_p > 1$ .

## 9. Experimental evidence on the coexistence of orthorhombic and tetragonal ferroelectric phases

An interesting feature of the lead-barium niobate solid-solution series is the fact that, over the composition range  $0.375 \leq x \leq 0.475$  the orthorhombic and tetragonal ferroelectric phases coexist in each compound. The electrical measurements referred to in Section 7 have shown that for each value of  $x$  in this range there is only one Curie temperature, and the two phases can therefore be regarded as ferroelectric polymorphs with approximately the same chemical composition. A high-temperature X-ray powder study of the two-phase composition  $x=0.4$  has confirmed this interpretation, and shows that both phases undergo structure transitions at a common Curie temperature. Thus, the orthorhombic component becomes tetragonal at temperatures above  $270^\circ\text{C}$ , while the tetragonal ferroelectric structure undergoes a discontinuous change in the  $a_T$  and  $c_T$  parameters, which must be attributed to the removal of a tetragonal strain from the pseudo-cubic perovskite units within the structure cell.

X-ray observations on single crystals grown from the melt, possessing the nominal composition  $x=0.4$ , show that the relative proportions of the two ferroelectric phases, and also the ferroelectric strain developed in the tetragonal phase, are very sensitive to firing temperature and crystal size. Thus, the effect of melting and crystallizing this compound was to increase the proportion of the tetragonal phase from about 15% to 50% of the whole, and slightly to increase its ferroelectric strain (i.e.  $c_p/a_p$  ratio).

Optical examination of crystals of composition  $x=0.4$  shows that they tend to grow with a columnar habit with the short (tetrad) axis lying parallel with the axis of the column. Many of the columns possess oriented overgrowths in the form of columns inclined at a constant angle of about  $71^\circ$  to the main crystal. By supplementing the optical studies with X-ray single-crystal oscillation photographs it was shown that the structures of the main column and the overgrowth correspond to those of the orthorhombic and tetragonal polymorphs respectively. Moreover, the

angle of overgrowth is found to agree almost exactly with that theoretically necessary to obtain a fit between the short axes of the two ferroelectric structures.

Some quite striking increases in ferroelectric strain were produced by rapidly melting and crystallizing single-phase tetragonal structures with nominal compositions  $x=0.5$  and  $0.6$ . The new values of  $c_p/a_p$  for these specimens are indicated in the graph, Fig. 7. The fact that no significant loss of weight was found to have occurred in these experiments suggests that these increases in axial ratio cannot be attributed to composition changes. It would appear that in the ceramic preparations the development of ferroelectric strain is inhibited by the small crystal size, which is generally about  $5\mu$ . Crystal growth permits an increase in  $c_p/a_p$  by reducing surface strain at the domain boundaries. Similar effects have been reported for  $\text{BaTiO}_3$  preparations of small crystal size by Anliker, Brugger & Känzig (1954).

## 10. Discussion

These studies have enabled the ferroelectric properties of  $(\text{Pb}, \text{Ba})\text{Nb}_2\text{O}_6$  and  $(\text{Ba}, \text{Sr})\text{Nb}_2\text{O}_6$  solid solutions to be explained in terms of the crystal structure, and indicate that the ferroelectricity of these structures is derived from the constituent perovskite-like groups of atoms within the structure.

It is probable that pure  $\text{PbNb}_2\text{O}_6$  possesses something of the character of a 'frozen-in' ferroelectric, in that its structure is too strained to permit of an easy reversal of the spontaneous polarization at normal applied field strengths. Replacement of Pb by Ba reduces this strain, and results in a progressive increase in the effective contribution to the ferroelectric behaviour. This effect may be compared with that found in certain perovskite-type ferroelectric solid solutions such as  $(\text{Pb}, \text{Ba})\text{ZrO}_3$  (Shirane & Hoshino, 1954),  $(\text{Na}, \text{Cd})\text{NbO}_3$  (Lewis & White, 1956) or  $(\text{Na}, \text{Pb})\text{NbO}_3$  (Franccombe & Lewis, 1957), where the replacement with Ba, Cd or Pb respectively reduces, or modifies, the lattice strain through changes in covalent bonding or puckering.

The existence of a minimum in the electrical Curie temperatures near the composition  $\text{Pb}_{0.5}\text{Ba}_{0.5}\text{Nb}_2\text{O}_6$  (see Fig. 6) can be attributed to a change in the type of ferroelectric strain within the crystal lattice. Thus, for compositions at the Pb-rich end of the system the perovskite-like structure units within the bronze-type unit cell are probably distorted in the same fashion as in orthorhombic  $\text{BaTiO}_3$ . At the Ba-rich end, however, (to the right of the Curie-point minimum in Fig. 6) these units are tetragonally distorted, owing to a relative expansion effect along the short axis of the bronze-type cell.

No detailed studies of the crystal structures of these ferroelectric compounds have yet been attempted, and the form adopted by the ionic displacements is

therefore not known. Nevertheless, from knowledge of the displacement of Ti atoms in the  $\text{BaTiO}_3$  structure one might conclude that below the Curie point the Nb atoms will be displaced relative to their oxygen octahedra along the axis of spontaneous polarization (or in the direction of ferroelectric strain). Thus, in the tetragonal ferroelectric phase the Nb displacements should occur in the  $[001]_p$  direction (Fig. 5(b)), i.e. along the  $c$  axis of the main structure cell. In the orthorhombic ferroelectric phase, however, the observed direction of spontaneous polarization is along the  $[110]$  axis of the ideal tetragonal (type I) cell (Franccombe & Lewis, 1958a). If the Nb displacements lie parallel with this axis, then they cannot also be directed along the face diagonals of the sub-units, and the analogy with orthorhombic  $\text{BaTiO}_3$  breaks down.

The more plausible explanation, in view of the obvious significance of the perovskite-like groups, is that the polar moment (and the Nb displacement) within each sub-unit lies along the  $[110]_p$  axis, as shown in Fig. 5(a). These Nb displacements can be resolved into components along (and at right angles to) the observed axis of spontaneous polarization for the main cell, i.e. from  $A$  to  $B$  in Fig. 5(a); the former components are parallel for all sub-units, the latter antiparallel. We now have to assign displacements to those Nb atoms which lie outside the perovskite sub-units, and are positioned at the mid-points of the edges of the type I unit cell, as shown in Fig. 2 of our earlier paper. If, as appears likely, they are displaced within their oxygen octahedra in the same way as we have suggested for the other Nb atoms, then they must move parallel with the  $[110]$  axis. This interpretation would attribute to  $\text{PbNb}_2\text{O}_6$ , and the iso-morphous Pb-rich phases in the  $(\text{Pb}, \text{Ba})\text{Nb}_2\text{O}_6$  system, a partly antiferroelectric character, and might account for the extreme difficulty experienced in reversing the polar moment. Structures containing individual dipole moments which are neither parallel nor antiparallel have been classed by Megaw (1957) as cone ferroelectrics; but these materials are still more general in that dipoles have to be assigned to two different kinds of octahedra, namely those in and those outside the perovskite-like sub-units.

Additional distortion effects appear to be present in the orthorhombic phases (Franccombe & Lewis, 1958a), associated with the puckering of Nb-O-Nb chains relative to the  $[001]$  axis, and in  $\text{PbNb}_2\text{O}_6$  itself these probably persist even above the Curie temperature, (Franccombe, 1958). The puckering of these chains in the orthorhombic structures is evidently a significant factor in determining the position of the orthorhombic-tetragonal phase boundary in the system  $(\text{Pb}, \text{Ba})\text{Nb}_2\text{O}_6$ . The transition to the tetragonal phase takes place when sufficient Pb has been replaced by Ba to allow the Nb-O-Nb chain along the  $b_m$ -axis of orthorhombic structure cell to straighten out. This occurs in the composition region  $0.375 < x < 0.475$ , where the observed discontinuous change in the mono-

clinic  $b_m$  parameter is associated with a switch of the polar moment in the perovskite sub-unit from the  $[110]_p$  to the  $[001]_p$  axis.

For each compound in the two-phase region near  $x=0.425$  the orthorhombic and tetragonal structures have a common Curie point, and presumably possess about the same free energy. An important feature of these phases, however, is that neither can transform directly into the other in a fashion analogous to the orthorhombic-tetragonal phase change occurring in  $\text{BaTiO}_3$  at 0 °C. In the pseudo-cubic perovskite ferroelectrics the phase change proceeds fairly smoothly by a switch in the direction of the polar moment from the  $[110]$  axis to the nearest cube edge. A similar change is not likely to take place in the bronze structure, since if the strain effect in each small perovskite unit switched from the  $[110]_p$  direction to one of the adjacent  $a_p$ -axes, this would give rise to an overall crystal symmetry lower than tetragonal. A change of strain direction from  $[110]_p$  to the third, more remote cube axis, that is the  $c_p$ -axis in Fig. 5(b), is improbable because it would involve a relatively large energy change. In other words the strain directions  $[110]_p$  and  $[001]_p$  are frozen into different domains, so that orthorhombic and tetragonal structures coexist.

The properties of the  $(\text{Ba}, \text{Sr})\text{Nb}_2\text{O}_6$  solid solutions appear to be very similar to those of the  $(\text{Pb}, \text{Ba})\text{Nb}_2\text{O}_6$  compounds. The scale of the ferroelectric distortion

effects is greatly reduced, however, compared with the  $(\text{Pb}, \text{Ba})$  series, this being consistent with the lower Curie temperatures. This difference is very reminiscent of that between  $\text{BaTiO}_3$  and  $\text{PbTiO}_3$ , and may very well be due to the same cause—the role of Pb.

### References

- ANLIKER, M., BRUGGER, H. R. & KÄNZIG, W. (1954). *Helvetica Physica Acta*, **27**, 99.
- COATES, R. V. & KAY, H. F. (1958). *Phil. Mag.* **3**, 1449.
- FRANCOMBE, M. H. (1956). *Acta Cryst.* **9**, 683.
- FRANCOMBE, M. H. (1958). Ph.D. Thesis, Univ. of London.
- FRANCOMBE, M. H. & LEWIS, B. (1957). *J. Electronics* **2**, 387.
- FRANCOMBE, M. H. & LEWIS, B. (1958a). *Acta Cryst.* **11**, 696.
- FRANCOMBE, M. H. & LEWIS, B. (1958b). Patent Application No. 1700/58.
- GOODMAN, G. (1953). *J. Amer. Ceram. Soc.* **36**, 368.
- GOODMAN, G. (1957). U.S. Patent No. 2,805,165.
- LEWIS, B. & WHITE, E. A. D. (1956). *J. Electronics*, **1**, 646.
- MAGNÉLI, A. (1949a). *Ark. Kemi Min. Geol.* **1**, No. 22.
- MAGNÉLI, A. (1949b). *Ark. Kemi Min. Geol.* **1**, No. 32.
- MEGAW, H. D. (1957). *Ferroelectricity in Crystals*, p. 16. London: Methuen.
- ROTH, R. S. (1957). *Acta Cryst.* **10**, 437.
- ROTH, R. S. (1959). Amer. Phys. Soc. Meeting, New York.
- SHIRANE, G. & HOSHINO, S. (1954). *Acta Cryst.* **7**, 203.

*Acta Cryst.* (1960). **13**, 140

## Defects in the Crystal and Magnetic Structures of Ferrous Oxide

By W. L. ROTH\*

General Electric Research Laboratory Schenectady, New York, U.S.A.

(Received 19 March 1959 and in revised form 21 April 1959)

The defect structure of non-stoichiometric  $\text{FeO}$  (Wüstite) has been investigated by measuring the neutron scattering of powders quenched from the high temperature equilibrium state. The nuclear scattering shows the defects to consist of both cation vacancies in octahedral sites and interstitial cations in tetrahedral sites. The defects give rise to diffuse scattering which suggests the atomic arrangement in the vicinity of the defect is similar to that in magnetite. The average magnetic moment of iron atoms in normal positions, obtained by measuring the scattering of neutrons by the periodic arrangement of spins in the antiferromagnetic state, indicate the magnetic structure in the vicinity of the defect is paramagnetic. The model is supported by magnetic studies which demonstrated the existence at low temperature of a magnetic remanence in exchange contact with the antiferromagnetic structure.

The magnetic structures of  $\text{MnO}$ ,  $\text{FeO}$ ,  $\text{CoO}$  and  $\text{NiO}$  have been studied by neutron diffraction with emphasis directed toward understanding their relation to the crystal anisotropies and deformations which occur on magnetic ordering (Shull *et al.* 1951; Roth, 1958).

The neutron scattering from ferrous oxide exhibits anomalies which are related to a defect structure, and they have been investigated further to ascertain the nature of the defects and their effects on the magnetic arrangement.

When equilibrium compositions of ferrous oxide are quenched to room temperature, a cubic (Wüstite) phase is formed in which the  $\text{Fe}/\text{O}$  ratio varies over

\* The neutron diffraction studies were carried out at the Brookhaven National Laboratory, Upton, L.I., New York.